

BUNCH MERGING AND COMPRESSION: RECENT PROGRESS WITH RF AND LLRF SYSTEMS FOR FAIR

D. E. M. Lens*, R. Balß, H. Klingbeil¹, U. Laier, J. S. Schmidt, K. G. Thomin,
 T. Winnefeld, B. Zipfel, GSI, Darmstadt, Germany
¹also at Technische Universität Darmstadt, Darmstadt, Germany

Abstract

Besides the realization of several new RF systems for the new heavy-ion synchrotron SIS100 and the storage rings CR and HESR, the FAIR project also includes an upgrade of the RF systems of the existing accelerator rings such as SIS18. The SIS18 RF systems currently comprise two ferrite cavities, three broadband magnetic-alloy cavities and one bunch-compressor cavity. In addition, the low-level radio frequency (LLRF) system has been continuously upgraded over the past years towards the planned topology that will be implemented for all FAIR ring accelerators. One of the challenges for the SIS18 RF systems is the large RF frequency span between 400 kHz and 5.4 MHz. Although the SIS18 upgrade is still under progress, a major part of the functionality has already been successfully tested with beam in machine development experiments (MDE). This includes multi-harmonic operation such as dual-harmonic acceleration and further beam gymnastics manipulations such as bunch merging and bunch compression. Many of these features are already used in standard operation. In this contribution, the current status is illustrated and recent MDE results are presented that demonstrate the capabilities of the RF systems for FAIR.

INTRODUCTION

During the past years, the low-level radio frequency (LLRF) system at the heavy-ion synchrotron (Schwer-Ionen Synchrotron) SIS18 has been gradually upgraded towards the planned LLRF topology [1] for the Facility for Antiproton and Ion Research (FAIR).

The currently available radio frequency (RF) cavity systems with selected technical parameters that are currently used during standard machine operation are summarized in Table 1, where N denotes the number of cavities of the given type in the ring. Besides cavities loaded with ferrite ring cores, magnetic alloy (MA) cavities have been installed that enable, among other scenarios, a dual-harmonic acceleration. In addition, a bunch compressor cavity (BC) has been commissioned for a fast bunch rotation in longitudinal phase space before extraction [2].

The revolution frequency in SIS18 varies between 215 kHz and 1.36 MHz and typical harmonic numbers are $h = 2$ for the MA cavities and $h = 4$ for the ferrite cavities. Nevertheless, a variety of other harmonic numbers (e. g. $h = 1, \dots, 8$) has been used for different scenarios and beam manipulations. The LLRF system has been designed to cope

with this flexibility, including changes of harmonic numbers at dedicated White Rabbit (WR) timing events. Particular challenges are the large frequency span, fast ramping rates of the RF frequency of at least 10 MHz/s, and a required phase and amplitude accuracy under dynamic conditions of $\pm 3^\circ$ and $\pm 6\%$, respectively.

Table 1: SIS18 RF Cavity Systems

Type	N	RF frequency	Typical voltage per cavity
Ferrite	2	800 kHz - 5.4 MHz	up to 14 kV _p
MA	3	400 kHz - 2.7 MHz	up to 13 kV _p
BC	1	800 kHz - 1.2 MHz	30 kV _p

At SIS18, the cavity systems produce single-harmonic RF voltages and multi-harmonic operation is realized by operating different systems at different harmonic numbers. In contrast to multi-harmonic cavity systems (e. g. [3]), the local signal generation for one cavity is therefore simpler, but the complexity of the higher-level LLRF is higher. In the following, we demonstrate the status and performance of the SIS18 LLRF systems.

SIS18 LLRF TOPOLOGY

A simplified diagram of the LLRF topology of SIS18 is shown in Fig. 1 with an emphasis on the cavity synchronization that ensures a synchronization of the gap voltages of all involved RF cavity systems (which may be configured to different harmonic numbers) in frequency and phase. The main signal sequence is as follows: The measured gap voltages are transmitted from the accelerator tunnel to the RF supply area.¹ In the supply area, the gap signals are distributed to a Switch Matrix. This matrix also receives reference signals from Group DDS (direct digital synthesis) modules that are based on clock signals of the bunch phase timing system (BuTiS, cf. [4]). At SIS18, four such modules exist ($i \in \{A, B, C, D\}$) that are configured independently with a harmonic number h_i , such that each module generates a reference signal with frequency $f_{RF,i} = h_i \cdot f_R$ as a multiple of the revolution frequency f_R . A phase calibration eliminates remaining phase errors between the analog output signals of the Group DDS [5].

Via equally structured signal paths using lines of the same type that have been assembled to a specified electrical delay, it is ensured that all input signals of the Switch Matrix have

¹ For FAIR, a signal transmission via optical and via coaxial lines is planned. At SIS18, the coaxial lines are currently the main transmission path.

* d.e.m.lens@gsi.de

Content from this work may be used under the terms of the CC BY 4.0 licence (© 2022). Any distribution of this work must maintain attribution to the author(s), title of the work, publisher, and DOI

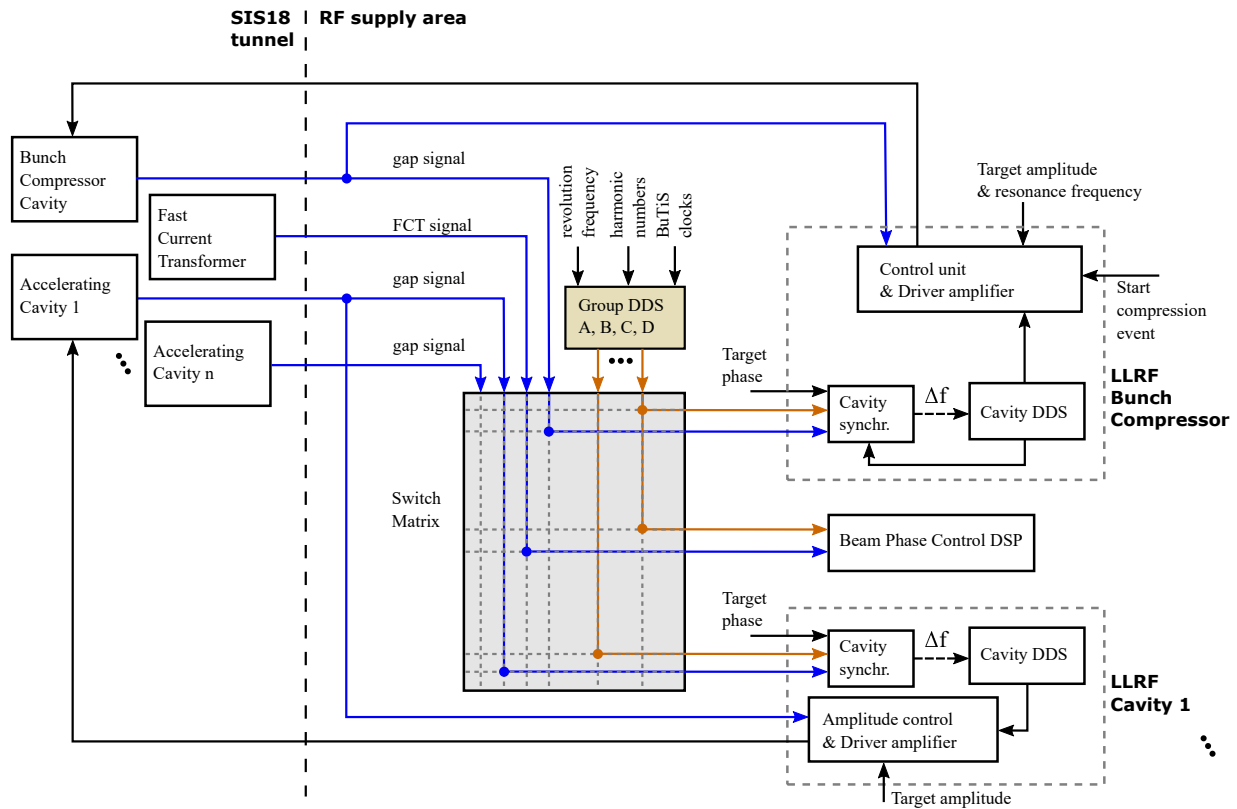


Figure 1: SIS18 LLRF topology with the cavity synchronization for the bunch compressor and one accelerating cavity (ferrite or MA). Some LLRF subsystems are omitted, e. g. the resonance frequency tuning loop for the ferrite cavities and calibration subsystems.

the same delay and can thus be compared with respect to the phase. This has been implemented for most lines of the SIS18 LLRF. However, some lines (such as the Group DDS delay lines) still have to be harmonized, because they are not yet of the correct type.

The Switch Matrix is configured such that a gap and a Group DDS reference signal with the same RF frequency $f_{RF,i}$ are selected and transmitted to the local LLRF subsystem of the respective cavity system. Depending on the phase difference of both signals, the cavity synchronization system corrects the local Cavity DDS with a frequency offset Δf . This eventually leads to a phase shift of the driver amplifier output signal (and thus the gap signal) until the phase between the gap and reference signal equals the target phase. The cavity synchronization also includes a (cavity) calibration to eliminate remaining, inevitable frequency-dependent amplitude and phase errors [6].

For the BC system, the synchronization topology is slightly different, as shown in Fig. 1. Since it is a pulsed system that has to deliver the RF peak voltage within a few tens of microseconds, its cavity synchronization system uses the Cavity DDS signal instead of the gap voltage. This has the advantage that the synchronization loop can already lock on the corresponding Group DDS signal before the start of the compressor pulse. Of course, the drawback of this procedure is that the subsequent subsystems (control unit, driver

amplifier and cavity including power amplifier) are operated in a feedforward manner, which makes a calibration curve for the target phase mandatory.

BUNCH MERGING

Bunch merging experiments have turned out to be a suitable benchmark scenario to test the overall phase accuracy of the SIS18 RF systems. On December 19th, 2019, a 8:4:2 merging was performed at SIS18 with about 1 mA of $^{40}\text{Ar}^{18+}$ ions on flat-top at 130 MeV/u ($f_R = 663$ kHz) with one ferrite cavity at $h = 8$ and two MA cavities at $h = 4$ and $h = 2$, respectively.

The merging scenario was fully controlled by the Central Control System (CCS), only the phase ramps were trimmed manually to optimize the two merging processes (8:4 and 4:2). First of all, the first merging was optimized by trimming the target phase of the cavity with $h = 8$. Afterwards, the target phase of the cavity with $h = 2$ was trimmed to achieve an optimized second merging. The resulting waterfall plot is shown in Fig. 2.

Figure 3 shows the optimization of the second merging 4:2 between the two MA cavities, where the target phase of the cavity with $h = 2$ was varied. A phase offset of a few degrees influenced the symmetry of the merging process noticeably. The best result was obtained for a phase offset of -3° with respect to the default CCS settings. Since this

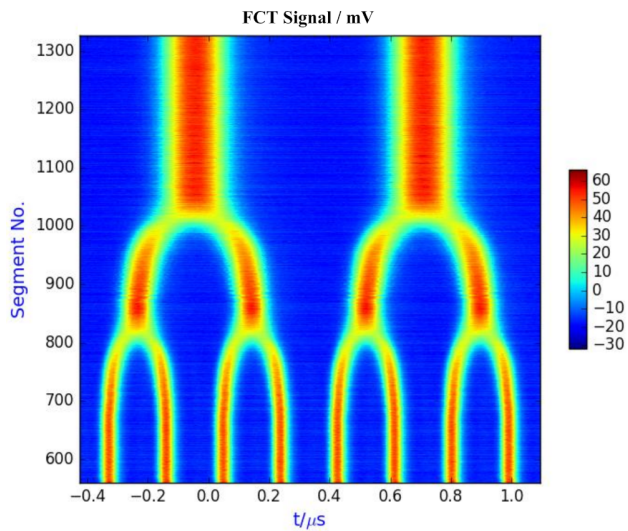


Figure 2: Waterfall plot of FCT signal after optimization of the two bunch merging sequences.

was close to the CCS default value, this is an indication that the cavities that were involved in this merging process had achieved the required phase accuracy of $\pm 3^\circ$.

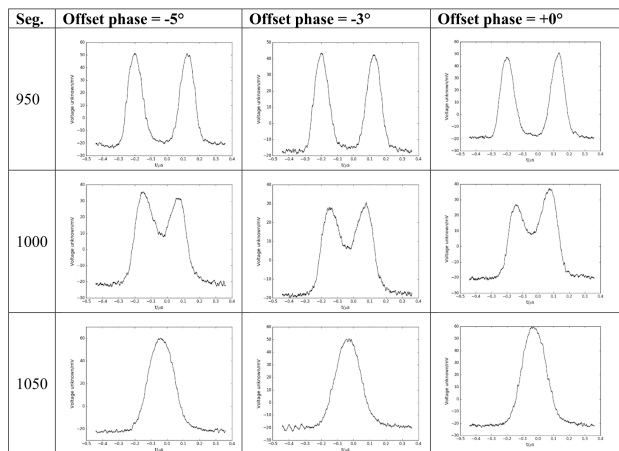


Figure 3: Optimization of 4:2 merging: FCT signal of two bunches merging into one (from top to bottom row) depending on the offset phase of the cavity with $h = 2$ (right column: default CCS settings with 0° offset).

The optimized first merging is shown in Fig. 4 as mountain range plot. It needed a much larger phase offset of 25° for the target phase of the ferrite cavity at $h = 8$. Although it can be expected in general that some systematic errors such as signal delay differences will be multiplied by the harmonic number at which the cavity system is operated, and therefore higher phase offsets may occur at higher harmonic numbers, this clearly is beyond the required accuracy. The precise error source is still under investigation, but since the LLRF upgrade at SIS18 has not yet been fully implemented, it is expected that the remaining phase errors can be decreased further. In particular, there are still some remaining unequal-

ities in the signal distribution lines between the ferrite and MA cavity systems that have to be harmonized.

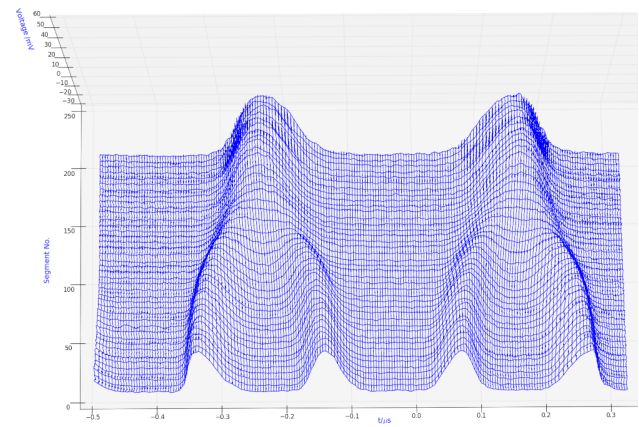


Figure 4: Mountain range plot of the FCT signal for the optimized 8:4 merging (segments 700 to 900) with phase offset $+25^\circ$ for the ferrite cavity with $h = 8$.

BUNCH COMPRESSION

The SIS18 bunch compressor was re-commissioned with beam in 2021 with the new FAIR control system based on LSA and FESA [7, 8]. In the MDE that took place on June 13th, 2021, a single bunch was compressed on flattop before fast extraction. The main parameters of the experiment are summarized in Table 2.

Table 2: MDE Bunch Compression Parameters (Flattop)

Parameter	Value
Ion species	40Ar^{18+}
Cavities used	2 (1 MA and 1 BC)
Energy	300 MeV/u
Rev. frequency	904.9 kHz
Harmonic number	$h = 1$
Beam current (typ.)	2.75 mA
RF voltage	760 V_p (MA), 30 kV_p (BC)

A beam phase control (BPC) system as shown in Fig. 1 was used to tune the target phase for the bunch compressor system during commissioning with beam. The BPC was operated in open loop² and allowed the measurement of the beam phase with respect to the Group DDS signal at $h = 1$ during the bunch compression. By minimizing the beam phase variation during compression, the target phase could be calibrated efficiently. The resulting waterfall plot of the FCT beam signal is shown in Fig. 5. The measurement was triggered by a dedicated WR timing event, which also triggered the start of the bunch compressor voltage pulse with a (configurable) delay of $240\ \mu\text{s}$. Note that in this experiment, the beam extraction was intentionally set to an instant of time after the point of maximum compression to

² The feedback for damping coherent bunch oscillations was switched off.

Content from this work may be used under the terms of the CC BY 4.0 licence (© 2022). Any distribution of this work must maintain attribution to the author(s), title of the work, publisher, and DOI

study the compression in detail. Of course, during standard operation, the extraction would have to take place earlier.

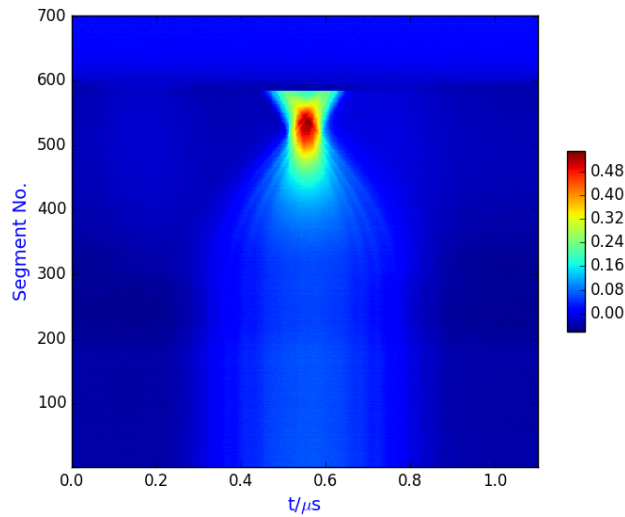


Figure 5: Waterfall plot of FCT signal for the bunch compression with extraction near segment 600. Each segment corresponds to one revolution period ($T_R = 1.1 \mu s$).

Figure 6 shows the obtained bunch profiles before and at maximum compression. From these profiles, a full width at half maximum (FWHM) value of 410 ns before compression and of 67 ns at highest compression is obtained. This leads to a compression factor of

$$K_{CF,achieved} = \frac{410 \text{ ns}}{67 \text{ ns}} \approx 6.1,$$

which is close to the theoretical value of

$$K_{CF,theory} = \sqrt{\frac{\hat{V}_{BC+MA}}{\hat{V}_{MA}}} = \sqrt{\frac{30 \text{ kV}_p + 760 \text{ V}_p}{760 \text{ V}_p}} \approx 6.4.$$

Thus, the compression efficiency was almost ideal during the experiment.

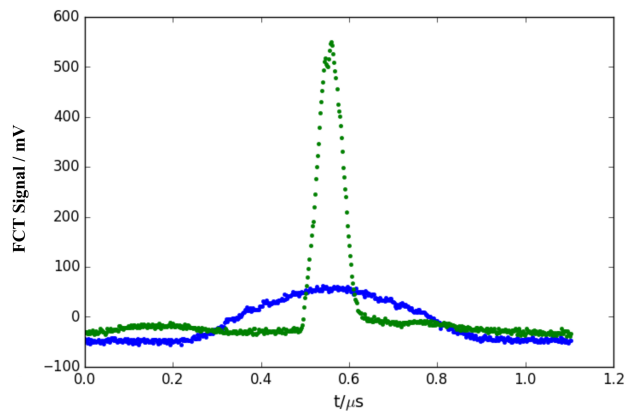


Figure 6: Comparison of bunch profiles before (blue) and at maximum compression (green).

The amplitude of the bunch compressor voltage is shown in Fig. 7. The voltage starts rising shortly after the set delay of 240 μs and reaches the maximum value after 40 μs .

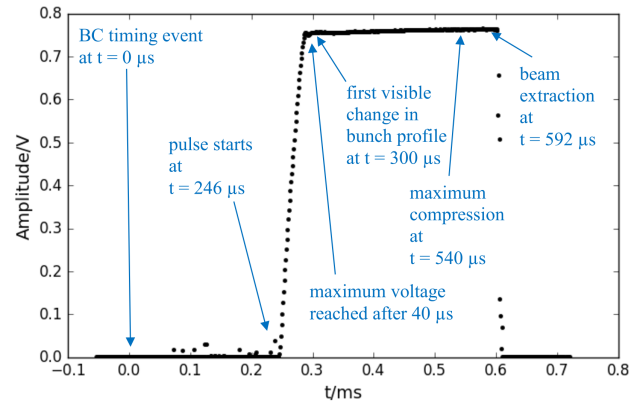


Figure 7: Bunch compressor voltage amplitude, scale 1:40,000 (obtained by a sine fit algorithm on the measured gap voltage signal; the smaller outliers before the pulse are numerical artefacts of the sine fit).

CONCLUSION AND OUTLOOK

Although many important aspects of the FAIR LLRF topology have been installed at SIS18, still a lot of effort has to be invested during the following years to reach the full functionality for the users. This includes the full control system integration of the bunch compressor cavity, the Switch Matrix, and the beam phase control loop. In addition, some subsystems and signal distribution channels of the older ferrite cavity systems have to be harmonized with the newer systems to reach the required phase accuracy for all SIS18 RF systems. Also, a driver amplifier upgrade of the MA systems is planned to decrease the energy consumption. Finally, an LLRF system that distributes optical phase and frequency corrections to the Group DDS modules is needed in order to enable manipulations of higher-level systems such as beam phase control, RF knock-out extraction, and full features of the new bunch-to-bucket transfer system in standard operation.

ACKNOWLEDGEMENTS

The authors would like to thank A. Andreev, P. Hülsmann, A. Klaus, H. G. König, K.-P. Ningel, D. Penza, A. Stuhl, C. Thielmann, and S. Schäfer for many technical contributions to the RF and LLRF systems. For the organization and approval of beam time, we would like to thank in particular P. Spiller, J. Stadlmann, and S. Reimann. We are also grateful for the help of several individuals from different GSI departments (e. g. ACO, SYS, BEA, OPE). This includes (but is not limited to) R. Bär, D. Beck, P. Kainberger, H. Liebermann, D. Ondreka, and H.J. Reeg.

REFERENCES

- [1] H. Klingbeil *et al.*, “New digital low-level rf system for heavy-ion synchrotrons”, *Phys. Rev. ST Accel. Beams*, vol. 14, no. 5, p. 102802, 06.10.2011.
doi : 10.1103/PhysRevSTAB.14.102802

- [2] P. Hülsmann, R. Balß, H. Klingbeil, and U. Laier, “Bunch Compression for FAIR”, in *Proc. 23rd Particle Accelerator Conf. (PAC’09)*, Vancouver, Canada, May 2009, paper TU5PFP023, pp. 864–866.
- [3] P. Ausset *et al.*, “A High-Power Multiple-Harmonic Acceleration System for Proton- and Heavy-Ion Synchrotrons”, in *Proc. 16th Particle Accelerator Conf. (PAC’95)*, Dallas, TX, USA, May 1995, paper WPQ26, pp. 1781-1784.
- [4] B. Zipfel and P. Moritz, “Recent Progress on the Technical Realization of the Bunch Phase Timing System BuTiS”, in *Proc. 2nd Int. Particle Accelerator Conf. (IPAC’11)*, San Sebastian, Spain, Sep. 2011, paper MOPC145, pp. 418–420.
- [5] A. Andreev, H. Klingbeil, and D.E.M. Lens, “Phase Calibration of Synchrotron RF Signals”, in *Proc. 8th Int. Particle Accelerator Conf. (IPAC’17)*, Copenhagen, Denmark, May 2017, pp. 3945–3947.
doi:10.18429/JACoW-IPAC2017-THPAB097
- [6] U. Hartel *et al.*, “Precise Verification of Phase and Amplitude Calibration by means of a Debunching Experiment in SIS18”, in *Proc. 4th Int. Particle Accelerator Conf. (IPAC’13)*, Shanghai, China, May 2013, paper THPEA004, pp. 3155–3157.
- [7] R. Mueller *et al.*, “Supporting Flexible Runtime Control and Storage Ring Operation with the FAIR Settings Management System”, in *Proc. ICALEPCS’21*, Shanghai, China, Oct. 2021, pp. 768–773.
doi:10.18429/JACoW-ICALEPCS2021-WEPV047
- [8] R. Huhmann *et al.*, “The FAIR Control System - System Architecture and First Implementations”, in *Proc. 14th Int. Conf. on Accelerator and Large Experimental Physics Control Systems (ICALEPCS’13)*, San Francisco, CA, USA, Oct. 2013, paper MOPPC097, pp. 328–331.